Silicon (2022) 14:10521–10534
https://doi.org/10.1007/s12633-021-01648-6

ORIGINAL PAPER

Fabrication of effective mesoporous silica materials for emergency hemostasis application

Zhuoran Zhang · Tao Liu · Zenghua Qi · Fan Li · Kun Yang · Sheng Ding, et al. *[full author details at the end of the article]*

Received: 19 October 2021 / Accepted: 28 December 2021 / Published online: 11 March 2022

Abstract
Uncontrolled bleeding is an important cause of traumatic death in wartime and peacetime. Despite the significant advances in hemostatic research, it is still challenging to develop safer and more effective hemostatic agents or dressings for emergency hemostasis application. Herein, we present a mesoporous silica particle (MSP) with large mesopores (12 nm around) through a facile and relative mild approach using dual silica source. The whole blood clotting time of MSP was about 23.13% shorter than that of Celox™ Granules (chitosan powder, a famous hemostatic agent) in vitro. To further facilitate the practical use in emergency hemostasis, MSP was fixed on cotton fibers by in-situ synthesis to form the composites of mesoporous silica-cotton (MS-C). The mass fraction of mesoporous silica reached 12.05% in MS-C, and the MSP are firmly anchored onto the cotton surface with < 5% leaching after 10 min of sonication. Both MSP and MS-C showed excellent biocompatibility in cytotoxicity tests of L-929 cells. Finally, the practical hemostatic effect of these mesoporous silica materials was preliminarily tested on the mouse tail truncation hemorrhage model, MS-C showed even shorter blood clotting time (86.00 s) and less blood loss (0.02 g) than that of MSP (172.30 s, 0.07 g), besides the less residue and a cleaner wound surface. It was probably that MS-C had great potential for emergency hemostasis applications.

Keywords Mesoporous silica · In-situ synthesis · Dual silica source · Hemostasis

1 Introduction

Uncontrolled bleeding and its serious complications were the leading cause of battlefield casualties and civilian trauma deaths [1–2]. Timely pre-hospital hemostasis will directly affect the infection rate and mortality rate. Therefore, various hemostatic agents or dressings had been developed for early and efficient control of the life-threatening hemorrhage. The ideal hemostatic dressing for pre-hospital applications should meet the following criteria[3–4]: (1) It can be directly used on bleeding wounds and can control the bleeding of large arteries and veins within 2 min; (2) No mixing or other preparations are required before use; (3) Easy to use, even non-medical personnel can use it skillfully; (4) Lightweight and durable; (5) It can still maintain stable properties in a wide temperature range (-10 ~ 50), long-term storage (at least 2 years of validity); (6) No risk of infection or tissue damage; (7) The price is economical, and it is easy to equip in large quantities.

Overall, domestic and foreign hemostatic agents or dressings can be divided into two categories: polymer and inorganic. Polymer hemostatic materials mainly include chitosan, cellulose, collagen and gelatin, fibrinogen [5–9]. The Celox series products are representative for polymer hemostatic materials based on chitosan. The common coagulation components of inorganic materials are zeolite, kaolin, and montmorillonite. QuikClot Combat Gauze (CG, kaolin-coated gauze) [10–12] and WoundStat (WS, smectite mineral powder) were the second-generation products recommended by the Committee on Tactical Combat Casualty Care (CoTCCC) for use in pre-hospital situation to minimize hemorrhage. WS appears to be the most efficacious agent, followed closely by CG and Celox. It seemed that the hemostatic efficiency and environmental adaptability of inorganic hemostatic materials are better than that of polymer materials. Although these products showed more significant hemostatic efficiency than the classical medical cotton gauze, they have some adverse side effects that cannot be neglected, such as abnormal foreign-body reactions, thermal tissue injuries, and so on [13].

Generally, the sudden trauma after the emergency hemostasis treatment pre-hospital needs a further debridement latter, which is different from the hemostatic

operation finished in operating room. Hence the hemostatic agents or dressings for emergency hemostasis application should not only be effective for use, but also safe and easy to remove. There are kinds of powder type hemostatic materials [14] successfully used for control of hemorrhage. However, most of them were easy to cause unclean wounds and residual problems, even the dangerous thrombosis once transferred in the blood vessels, all of which would lead to secondary damages [15–19].

Recently, mesoporous silica materials [20–22] with controllable composition and similar microstructures have drawn the close attention of many scholars, and it has shown infinite potential for pre-hospital hemostatic applications [23]. Malmberg et al. [24] reported that exposure of blood to materials with varying pore sizes in the micrometer regime greatly affects subsequent cellular adhesion and growth. Xv et al. [25] compared the hemostatic performance and exothermic reaction law of the mesoporous material HW with different pore diameters and the microporous material ZSM-5, and believed that the mesoporous material HW has faster hemostatic performance and lighter radiation than the microporous material ZSM-5. Baker et al. [26]. have determined that material cell-window size variations in the nanometer range greatly affect the clotting activity. It has been reported that mesoporous silica materials with larger pore diameters had better blood coagulation effects [27]. In the typical synthesis route of mesoporous silica, different templates were commonly used to form desired mesopores, and the high-temperature calcination method is commonly used to remove the template [28–31]. The calcination treatments dictated that it was difficult for mesoporous silica to bind with other flexible support materials through in-situ synthesis.

Cotton is most commonly processed into sterile gauze as a clinical sanitary consumable, attributing to its superiorities of strong adsorption, flexible structure, good biological safety and low cost. Cotton is almost entirely composed of cellulose [32], and cross-linked cotton fibers could form a flexible 3D mesh matrix with a strong water-absorbing surface [33]. The cellulose is a polyol [34], each of its structural units contains three unbound OH groups with different chemical activities, which form hydrogen bond chains between cellulose. And the hydrogen bonds in the cellulose recently were used to bind mesoporous single-crystal chabazite zeolite onto the surface of cotton fibers [35]. Hence mesoporous silica particle (MSP) has similar microporous structure to zeolite [36], but superior biocompatibility and functional scalability [37], it is likely to be a more desirable choice to combine MSP with cotton as an effective emergency hemostatic dressing. In this work, MSP was prepared through a facile and relative mild approach using dual silica source. To further facilitate the practical use in emergency hemostasis, MSP was loaded on cotton fibers by in-situ synthesis to form the composites of mesoporous silica-cotton (MS-C). The physical and chemical properties of MSP and MS-C were detected by TEM, SEM, XRD, FITR, TG, BET etc. The hemostatic properties were also studied by different in vitro blood clotting tests and preliminary animal trauma model trials.

2 Experiment

2.1 Chemical and reagents

All materials were analytical grade and used as received without further purification. Tetraethoxysilane (TEOS) was purchased from Kermel, sodium silicate solution (20% of SiO_2, 6% of Na_2O) was procured from Macklin. Triblock poly (ethylene oxide)-poly (propylene oxide)-poly (ethylene oxide) co-polymer Pluronic P123 (Mav = 5800, $EO_{20}PO_{70}EO_{20}$) and other reagents were obtained from Sigma-Aldrich Company. Medical absorbent cotton was purchased from Winner Medical Group. Celox™ Granules was purchased from Union Medical Supplies Company. QuikClot Combat Gauze (CG) was purchased from commercial source.

2.2 Preparation of mesoporous silica particle (MSP)

The mesoporous silica was prepared using P123 as the template, TEOS and sodium silicate as a mixed silica source [38]. In a typical synthesis, P123 and ethanol were dissolved in HAc-NaAc buffer solution (pH 4.4) at 25 under vigorous stirring. The ethanol/P123 molar ratio is 213. And then sodium silicate was added to the above solution. 10 min latter, TEOS was added. The molar ratio of the resulting gels was 100 SiO_2: 1.02 P123:85.2 acetic acid: 44.5 sodium acetate. The mixture was stirred at 40 for 20 h and followed a 24 h hydrothermal aging at 100 . Finally, the template in the product was washed by Soxhlet extraction [39] and dried to obtain MSP. The extracted MSPs were denoted as $(NaSi)_{100-x}E_x$, where x (x=30, 50) is the molar percent of TEOS/ (Na_2SiO_3 + TEOS), NaSi refers to Na_2SiO_3, and E refers to TEOS. By adjusting the initial molar ratio of TEOS/ (Na_2SiO_3 + TEOS) from 0 to 0.5, the pore size of the mesoporous silica can be adjusted.

2.3 Preparation of mesoporous silica-cotton (MS-C)

An in-situ synthesis method [40] was used to prepared composites of MS-C. The medical absorbent cotton was impregnated in acetone under ultrasonic conditions for a period of time and dried under 60 . Then the preprocessed cotton was directly put into the precursor gel which was

the same to that of MSP. After fully immersion, the cotton and precursor gel were transferred into a Teflon-lined stainless-steel autoclave. The same hydrothermal treatment and Soxhlet extraction were carried out to obtain the final MS-C. For contrast, the same process was carried out on the medical absorbent cotton without pretreatment, and the final product was named MS-C_0. The silicon source ratio of the precursor gel used in the above two samples was 1:1.

2.4 Characterization

2.4.1 Physical and chemical properties

FEI Tecnai F30 transmission electron microscope (TEM) was used to observe the morphology and pore structure of the sample. Zeiss Merlin Compact scanning electron microscope (SEM) was used to observe the particle load on the cotton fiber and the particle morphology. The samples were dried and sprayed with gold before testing. X-ray diffraction (XRD) patterns were recorded by the Bruker D8 Advance powder diffraction system, scanning from 0.5° to 10° at a speed of 0.5°/min. The nitrogen adsorption/desorption isotherms were performed on a Kantar autosorb-1 system at a temperature of 196 °C. The BJH (Barrett-Joyner-Halenda) method was used to calculate the pore size distribution curve of the adsorption/desorption branch. A Nicolet 380 infrared spectrometer from American Thermo Company was used for infrared spectroscopy analysis (FITR) with a resolution of 0.09 cm^{-1} and a scanning range of 4000-400 cm^{-1}. STA449F3 thermogravimetric (TG) analyzer was used to detect the loading rate of mesoporous silica particles on cotton fibers. The samples were heated to 800 °C from room temperature 5 °C/min under a dynamic oxygen flow. The sonication treatment was used to evaluate the binding strength between solid content and fabric by an ultrasonic cleaner (BUG25-06, Branson). The samples were added into deionized water and treated with sonication at different time intervals.

2.5 Determination of clotting activity in vitro

Blood samples came from New Zealand white rabbit (3-4 kg) which was collected and mixed with 3.8% trisodium citrate solution in a ratio of 9:1. This anticoagulated whole blood was kept at 4 for further use.

The clotting blood tests (CBT) [41] is a basic hemostatic test which can directly reflect and evaluate the hemostatic ability. CBT was started by adding 10 mg sample into 5 mL siliconized glass tubes and followed by incubating at 37ºC for 5 min. The control group added nothing. Then 1 mL citrated rabbit blood was mixed with the sample, and then continued for incubation at 37ºC for 3 min. After that, 500 μL of 0.025 mol/L $CaCl_2$ aqueous solution was added into the tube to trigger the coagulation pathway. Once the test tube was tilted up to 90° and there was no blood flow, the blood clotting time of each group was recorded. Each sample was repeatedly measured 3 times.

The clinical standard coagulation tests (prothrombin time (PT) and activated partial thromboplastin time (APTT)) [42] were performed using Mindray C2000-4 semi-automatic blood coagulometer. APTT can reflect the intrinsic coagulation pathway while PT is associated with extrinsic pathway. After centrifuging the anticoagulated whole blood at a speed of 3000 r/min for 10 min, the upper layer of plasma was taken for APTT and PT tests.

The sample and plasma were fully mixed according to the ratio of 2.5 mg sample to 100μL plasma. The APTT reagent and 50 μL supernatant were mixed and incubated at 37 for 5 min. After that, the 50 μL, 0.025 mol/L $CaCl_2$ solution was added to concentration, recording the time of plasma coagulation. Each sample was repeated 3 times.

Mixing the sample and plasma thoroughly in the same ratio as APPT. After standing, the 50 μL supernatant was incubated at 37 for 3 min. Recording the plasma clotting time after 50 μL PT reagent was added. Each sample was repeated 3 times.

Thromboelastograph Analyzer (TEG, CFMS LEPU-8800, China) was applied to assay the in vitro hemostatic activity of samples [42]. Before testing, the samples were dried at 80ºC to remove moisture. 10 mg of sample were added into 1 mL citrated rabbit whole blood. Using the vortex mixer to get the homogeneous mixture and then 340 μL of the mixture was added to the coagulation cup at 37ºC. Then after 20 μL of 0.2 mol/L $CaCl_2$ was also added to the coagulation cup, the coagulation cups were immediately tested to obtain the relevant parameters. Citrated rabbit whole blood without sample was used as a blank control group, and each group of samples was tested repeatedly three times.

2.6 Biocompatibility evaluation of mesoporous silica materials

The growth status of mouse fibroblast L-929 under different concentrations of sample conditions was used to analyze the impact of different doses of samples on cell biological safety. As to MSP, the high concentration of 100 μL, 640 μg/mL samples and the low concentration of 100 μL ,320 μg/mL samples were set. A normal culture control group and a solvent control group were setted up at the same time. As to MS-C and MS-C_0, the cytotoxicity was evaluated by examining the extract of samples in culture medium. All samples were soaked in the culture medium for 24 h, and then the extract solutions were diluted to different concentrations (100%, 50%

and 10%). After 24 h in a carbon dioxide incubator, 10 μL of CCK-8 solution was added. After incubating at 37 for 2 h, draw 100 μL of CCK-8-containing medium was drawn. The absorbance intensity was detected at 450 nm with the microplate reader.

The cell survival rate was calculated after the cells exposed to different concentration of extract solutions for 24 h. The other experimental steps were performed the same to that of MSP.

Staining of dead/live cell : The cells and the medium concentration were set in the same way. After discarding the original culture medium and washing the cells twice with PBS, the final concentration of 2 μ M Calcein AM and 4μ M EthD-I were added and mixed with 10ml PBS staining working solution respectively. 200μ L working solution was added to each well and incubated for 15 min in the dark at room temperature; Images of live (green fluorescence) and dead (read fluorescence) cells were obtained with the fluorescence microscope.

For MS-C type samples, the cell survival rate was calculated after the cells exposed to different concentration of extract solutions for 24 h. The other experimental steps were performed the same to that of MSP.

2.7 Hemostasis in Mouse tail truncation model

Mice (15, 33–39 g, male) [43] were randomly divided into 5 groups and used as mouse tail amputation model assay. The mice were anesthetized by intraperitoneal injection of 2 wt% lidocaine hydrochloride (50 mg/kg) and fixed on the surgical board. After the tail was sterilized, 2/3 of its length was cut down using surgical scissors. Free bleeding lasted for 3 s to ensure normal blood loss. Then, different samples were used to cover the wound, and the powder sample was covered with gauze. The successful hemostasis point was defined as no active bleeding within 10 min after the external force was removed. Record the corresponding hemostasis time and blood loss.

3 Results and Discussion

3.1 Mesoporous silica particle (MSP)

Through the TEM the pore size and structure of MSP can be seen directly through the TEM (Fig. 1). $(NaSi)_{50}E_{50}$ and $(NaSi)_{70}E_{30}$ showed highly ordered pore structure in the TEM images. As to $(NaSi)_{50}E_{50}$-426, it could see the rod-shaped particle structure and disordered pore structure, probably forming in the process of hole expansion that the orderly structure in the middle was destroyed. The mesoscopic structure of powder was characterized by XRD method (Fig. 2). All samples had diffraction peaks at 0.8°-2° and sharp peaks at 0.8°. These characteristic peaks could be indexed to the hexagonal symmetry lattice [44]. It is further proved that the mesoscopic structure of as-synthesized samples belongs to the two-dimensional hexagonal structure, which is the characteristic of typical mesoporous molecular sieves.

FTIR was used to detect the surface functional groups of samples. The Fourier infrared spectrum of the sample with three raw material ratios was shown in Fig. 3. The three groups of MSP samples have a broad absorption peaked at 3420 cm^{-1}, which was attributed to the stretching vibration peak of Si-OH and O-H in the adsorbed water. There were typical absorption vibration peaks of Si-O-Si bond at 1080 cm^{-1}, 806 cm^{-1}, and 461 cm^{-1}.

Nitrogen adsorption was used to characterize the pore size, specific surface area and pore volume of samples. Figure 4 showed the nitrogen adsorption/desorption isotherms of ($(NaSi)_{50}E_{50}$, $(NaSi)_{70}E_{30}$ and $(NaSi)_{50}E_{50}$-426. All the isotherms were all typical IV adsorption lines [45], indicating

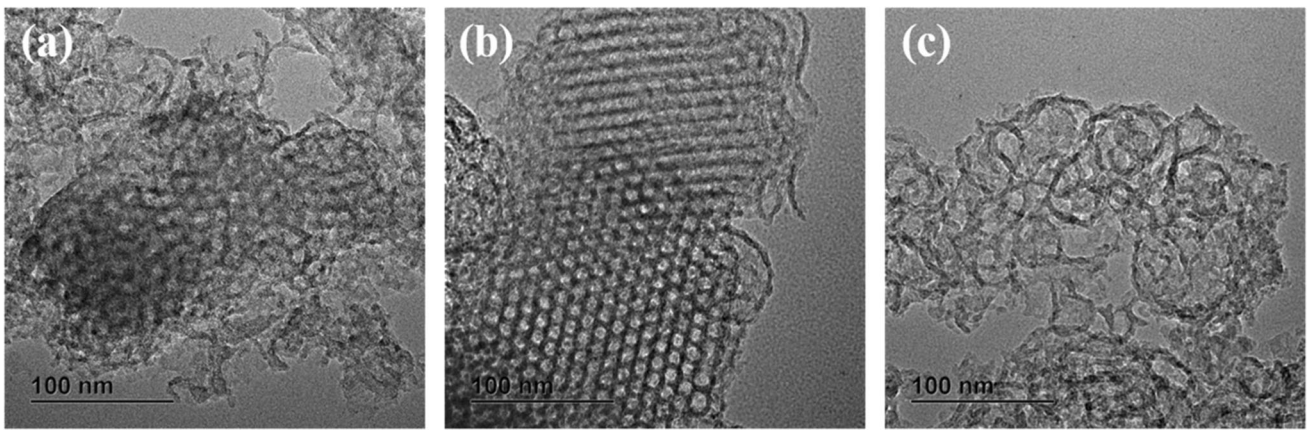

Fig. 1 TEM images of MSP with different raw material ratios: (**a**) $(NaSi)_{50}E_{50}$, (**b**) $(NaSi)_{70}E_{30}$, (c) $(NaSi)_{50}E_{50}$-426

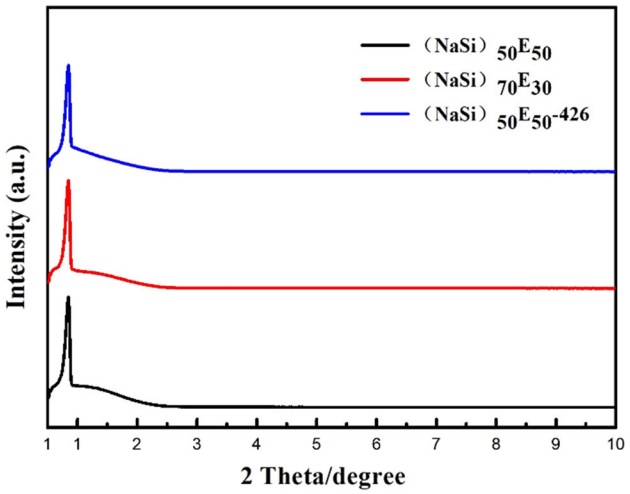

Fig. 2 XRD images of MSP with different raw material ratios

that the samples contained a large number of mesopores. Table 1 showed the pore size and other data of three samples, it can be seen clearly that under the same conditions of the solvent system, when the silica source ratio is 1:1, the sample pore size, specific surface area and pore volume were larger than the others. When the ratio of the silica source is the same, changing the ratio of the solvent system can increase the pore size. But in consideration of the TEM results, the group of $(NaSi)_{50}E_{50}$ has relatively large pore size and a stable microstructure.

The hemostatic performance of experimental samples in vitro was visually reflected through the CBT, as shown in Fig. 5. Compared with the blank control group (307.70 ± 12.50 s) and Celox™ (253.70 ± 10.02 s), all MSP samples can effectively shorten the hemostasis time and verify the excellent hemostatic performance of mesoporous silica materials; The CBT result of $(NaSi)_{50}E_{50}$ was 195.00 ± 2.60 s, which was about 23% shorter than that of Celox™

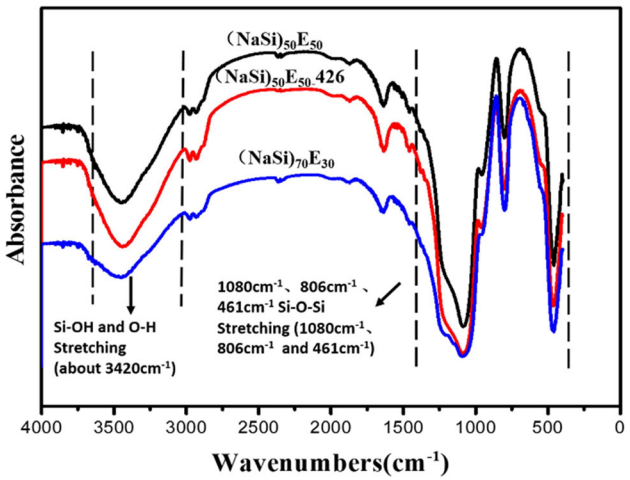

Fig. 3 FTIR images of MSP with different raw material ratios

Granules. $(NaSi)_{50}E_{50}$ with large pore size and stable structure showed the least hemostasis time in CBT, again indicating that the larger the pore size, the better the hemostatic effect of MSP.

APTT and PT are the two basic clinical coagulation tests in vitro. APTT reflects the endogenous coagulation pathway, while PT reflects the activation state of the exogenous coagulation pathway. The APTT and PT results were shown in Fig. 6. The APTT results showed that only $(NaSi)_{50}E_{50}$-426 (39.27 ± 2.54 s) had a significantly longer APTT value than the blank control group (21.90 ± 0.05 s), indicating that the endogenous coagulation factors in plasma were reduced and the procoagulant effect was not so good, which may be related to the broken mesoporous structure. The experience groups had no significant difference compared with the blank control group, which indicated that they had no significant effect on the endogenous coagulation pathway. The PT value of each group of samples decreased significantly compared with the blank control group (17.03 ± 1.26 s), indicating that the exogenous coagulation factors increased and the blood was in a hypercoagulable state, and mesoporous silica could activate the exogenous coagulation pathway. It was speculated that MSP could upregulate the expression of TF (Tissue Factor) [46, 47], which increases the blood viscosity and shortens the PT value.

TEG is an instrument for judging the effect of blood clotting by monitoring the changes in shear force during blood clotting. R, Angle and MA are the three most important parameters. The R value represents the time to start clotting, the Angle represents the coagulation rate, and the MA value represents the coagulation strength. Figure 6 showed the thromboelasticity diagrams of each group, and Table 2 showed the R, Angle and MA values detailly. It was clear that $(NaSi)_{50}E_{50}$ had the shortest time for blood coagulation initiation, the fastest coagulation rate and the nearly strongest blood clot intensity in all samples. Though the other two MSP samples also had shorter time for blood coagulation initiation, Celox™ showed its superiorities in faster coagulation rate and stronger blood clot intensity. The TEG results were mainly consistent with that of CBT, which not only showed the excellent hemostatic performance of mesoporous silica materials, but also verified again that the large mesoporous pore size can improve the hemostatic effect of MSP.

The ideal hemostatic material should have good biocompatibility. In this work, CCK-8 cytotoxicity tests and cell staining were used to detect the biocompatibility of different doses of MSP on L-929 mouse fibroblasts. According to reports [48], we used 320 μg/mL and 640 μg/mL as the low and high doses of MSP exposure, and 24 h as the exposure time. Figure 7 showed the cell survival curve of fibroblasts co-

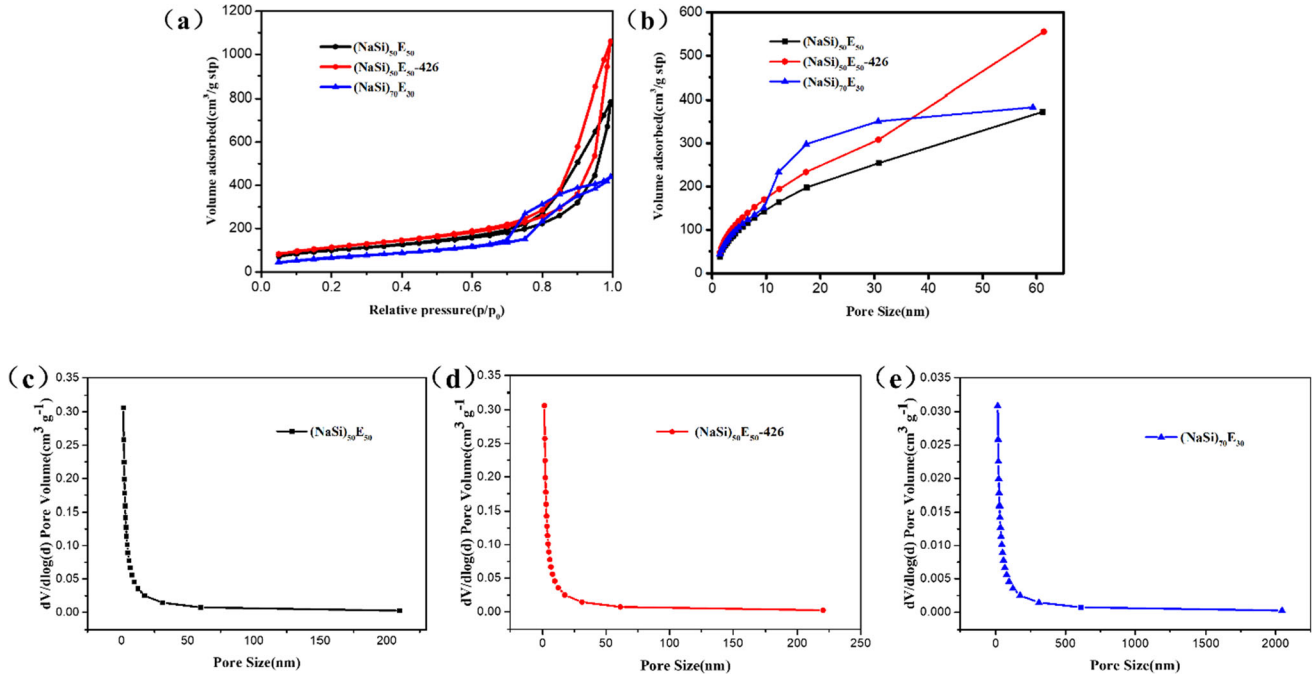

Fig. 4 (**a**) Nitrogen adsorption isotherms of MSP with different raw material ratios, (**b**) cumulative pore volume, (**c**)(**d**)(**e**) pore size distribution graphs measured by BJH method

cultured with different doses of MSP for 24 h. Both high and low doses had a certain inhibitory effect on cell growth. The cell survival rate of $(NaSi)_{50}E_{50}$-426 was a little weaker than the other two MSP samples. But the inhibition rate was considered acceptable, and all the cell survival rates were above 80%. It meant that MSP samples can meet the requirements of biological safety. The images of stained dead/live cells (Fig. 8) also showed clearly that there were more live cells (green) both at high and low doses for sample $(NaSi)_{50}E_{50}$ and $(NaSi)_{70}E_{30}$.

3.2 Mesoporous silica-cotton (MS-C)

SEM was used to visually examine the microstructure of as-prepared MS-C. It was found that the mesoporous silica particles were successfully loaded on cotton fibers, though the particle sizes were not regular. It was obviously that there were more particles on the cotton fibers that pretreated with acetone, comparing with that of sample MS-C_0 (Fig. 9).

The load percentage of MSP in MS-C was roughly evaluated by TG tests under a dynamic oxygen flow. As the trend shown in Fig. 10, MS-C had a relatively high load percentage of 12.05%, but the load percentage of MS-C_0 was 4.79%. The results of TG tests were consistent with the above SEM observation.

Table 1 The pore size, pore volume and specific surface area of MSP

Sample	BET surface area (m^2g^{-1})	Pore diameter (nm)	Total pore volume (cm^3g^{-1})
$(NaSi)_{50}E_{50}$	391.1	12.39	1.22
$(NaSi)_{50}E_{50}$-426	440.4	17.48	1.64
$(NaSi)_{70}E_{30}$	310.2	7.80	0.71

Calculated using the Barrett–Joyner–Halenda (BJH) model based on the desorption branch of the isotherm

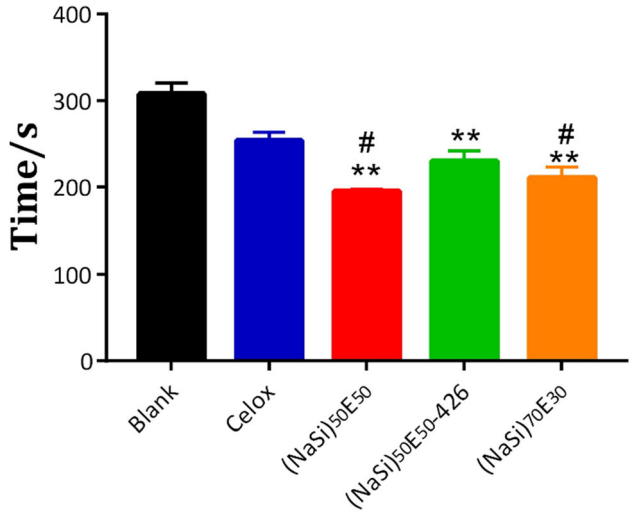

Fig. 5 In vitro clotting blood tests (CBT) of MSP with different raw material ratios, * and # indicate significant differences compared to the blank control group and the Celox group (**P<0.01)

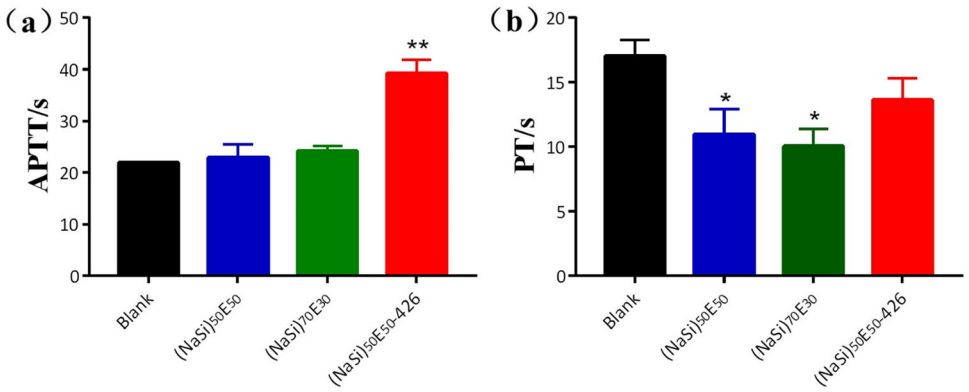

Fig. 6 The APTT and PT value of MSP with different raw material ratios, * indicates a significant difference from the blank control group(*P<0.05,**P<0.01)

As previously stated, it was a potential risk for the residues of powder type hemostatic materials in the wound. Here the binding strength between MSP and cotton fiber was evaluated by sonication treatment deionized water. The results showed there was less than 5% leaching MSP leached out from MS-C after 10 min sonication, but more than 80% of the kaolin particles leached out from the gauze. It revealed that the MSP particles were tightly bound onto the cotton fibers. The trend was shown in Fig. 11.

The nitrogen adsorption/desorption isotherm was used to characterize its microporosity and pore size (Fig. 12). The nitrogen adsorption isotherms of MS-Cs were all typical type IV isotherms of mesoporous structure, indicating that the particles on the cotton fibers had a mesoporous structure. Using the BJH method to calculate from the desorption distribution curve, the MSP pore size on MS-C_0 was 12.27 nm, while the MSP pore size on MS-C was 12.28 nm, which were closed to that of the pure MSP. The results of nitrogen adsorption tests showed that pretreatment of acetone did not affect the nucleation process of mesoporous silica.

The CBT in vitro had been used to intuitively reflect the hemostatic performance of the experimental sample (Fig. 13). The hemostatic time of MS-C (170.00 ± 9.16 s) was significantly shorter than that of MS-C_0 (224.00 ± 18.52 s). The results concluded that pretreatment of acetone can make it easy for mesoporous silica precursor gel to nucleate on the cotton fibers, thereby enhancing the hemostatic performance of MS-C.

The CCK-8 cytotoxicity results were shown in Fig. 14. There was no significant difference in cells survival rate of samples with different extract concentrations. Nearly all the results were above 90%, confirming the excellent biocompatibility of MS-C and MS-C_0. With careful examination and comparison (Fig. 16), it could be found that cytotoxicity of MS-C_0 was nearly not affected by the concentrations, and even it had a certain promotion effect on cell proliferation. As to MS-C, there was likely a bit inhibition effect on cell survival, which was conjectured that it may be related to the pretreatment using acetone. However, the cell survival rate could meet the biological safety requirements of hemostatic dressings.

Table 2 R, Angle, and MA values of the thromboelastogram (TEG) results

	R/min	Angle/deg	MA/mm
Blank	12.4 ± 0.95	36.6 ± 5.00	55.9 ± 11.41
Celox	6.7 ± 1.10	57.7 ± 7.27	73.5 ± 2.21
$(NaSi)_{50}E_{50}$	3.4 ± 1.06	65.1 ± 10.1	69.8 ± 8.08
$(NaSi)_{70}E_{30}$	3.7 ± 1.15	50.3 ± 5.29	55.1 ± 4.35
$(NaSi)_{50}E_{50}$-426	3.3 ± 0.56	51.0 ± 4.42	46.0 ± 6.29

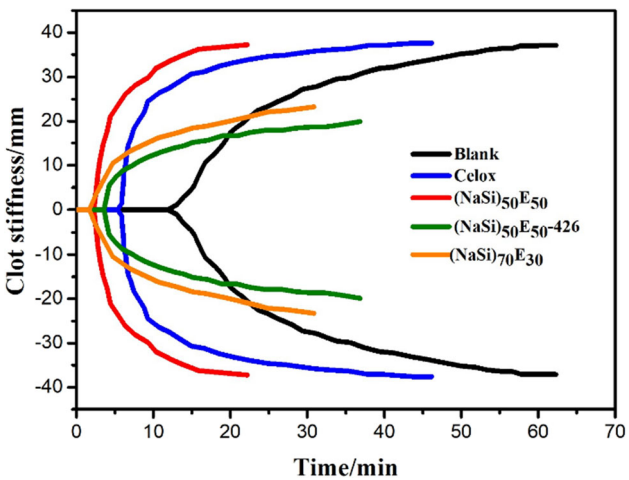

Fig. 7 Thromboelastogram (TEG) results of MSP with different raw material ratios

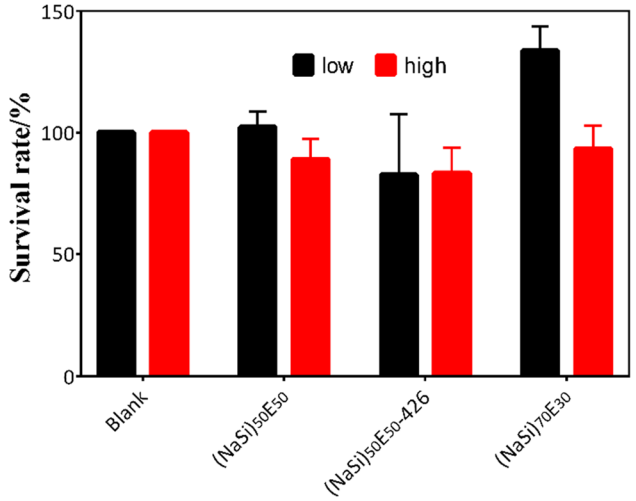

Fig. 8 Cell survival rate of different MSP at low(320 μg/mL) and high(640 μg/mL) concentration

3.3 Mouse tail truncation model

The mouse tail truncation model was established to intuitively evaluate the performance of MSP and MS-C in hemostasis. In the experiment, the hemostatic performance of each group was characterized by the cleanliness of the wound surface, the hemostasis time, and the amount of blood loss (shown in Fig. 15 and 18). After the bleeding being stopped, there was still powder residues found on the wound surface with treatment of MSP, while the wounds treated with MS-C and MS-C_0 were obviously cleaner. The average hemostatic time for MS-C (86.00 ± 36.76 s) and MS-C_0 (156.70 ± 15.63 s) were shorter than that of MSP (172.30 ± 4.16 s). As shown in Fig. 16, the average blood loss for MS-C_0 (28.10 ± 2.70 mg), MS-C (18.83 ± 3.60 mg) were significantly lower than MSP (67.90 ± 29.60 mg). It was concluded that MS-C with a large load of mesoporous silica

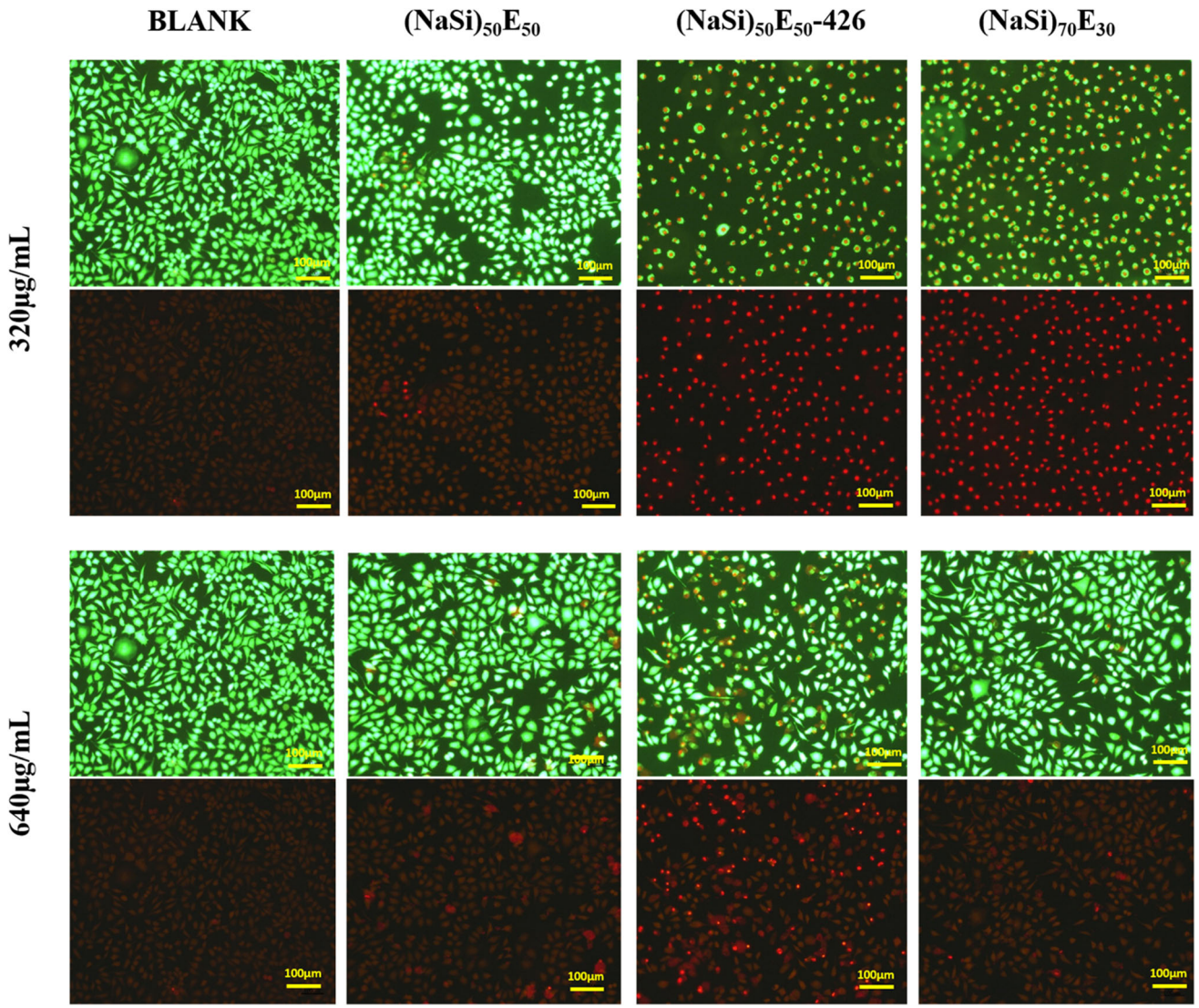

Fig. 9 Stained images of dead and living cells with different MSP at low(320 μg/mL) and high (640 μg/mL) doses

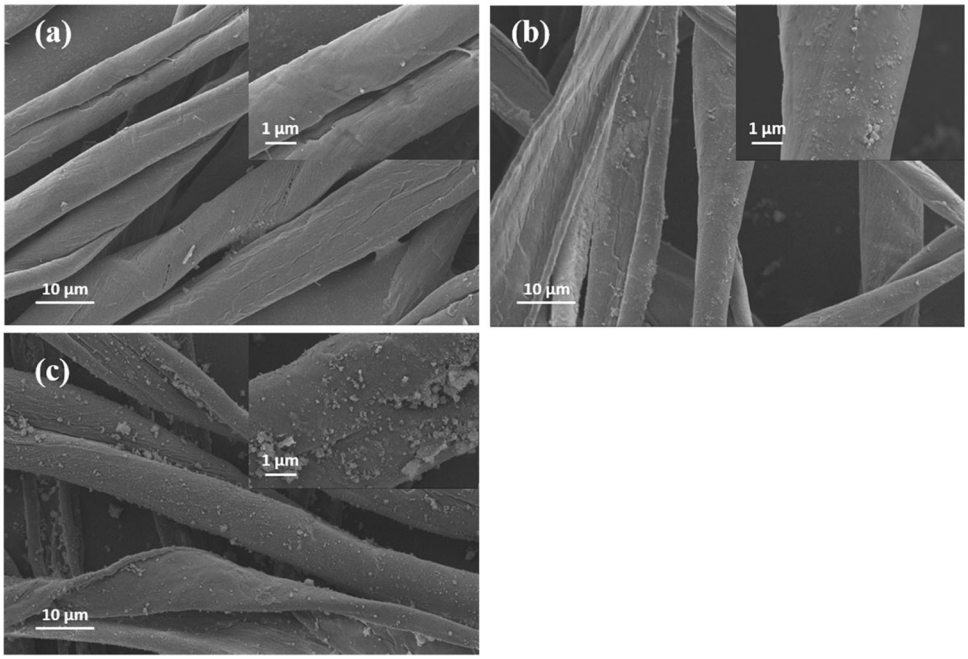

Fig. 10 SEM images of different samples: (**a**) cotton, (**b**) MS-C0, (**c**) MS-C. The inserted image is a partial enlargement

particles could not only bring about clean wounds, but also high hemostatic efficiency and excellent hemostatic effect.

4 Conclusions

In consideration of the complementary advantages of mesoporous silica and cotton, we prepared MSP with large mesopores through a facile and relative mild approach using dual silica source, and further MSP was fixed on cotton fibers by in-situ synthesis to form the composites of MS-C. The pore size of MSP was adjusted by the ratio of the two silica sources and the solvent system. MSP could activate the exogenous blood coagulation pathway, and the whole blood clotting time of MSP was about 23.13%, which was shorter than f Celox^{TM} in vitro. The mass fraction of mesoporous silica reached 12.05% in MS-C, and the MSP are firmly anchored onto the cotton surface with < 5% leaching after 10 min of sonication which was better than the CG (>80%). Both MSP and MS-C showed excellent biocompatibility in cytotoxicity tests of L-929 cells. The mouse tail truncation hemorrhage model tests revealed that MS-

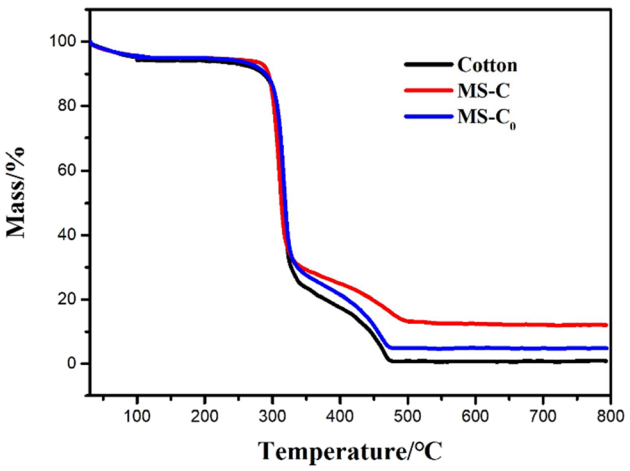

Fig. 11 Thermogravimetric (TG) analysis curves of different samples

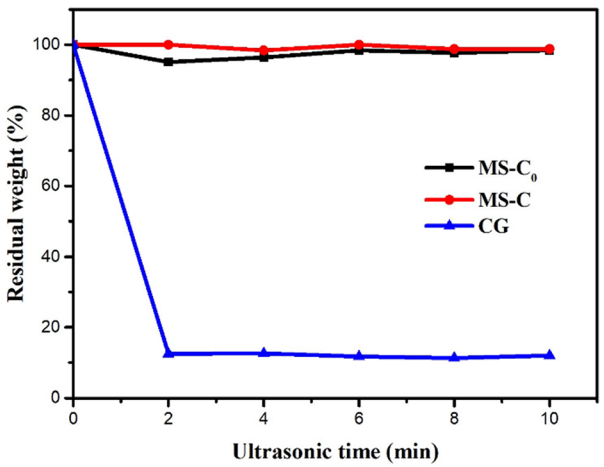

Fig. 12 The relative residual weight of hemostatic components on MS-C, MS-C_0, CG after different ultrasonic time

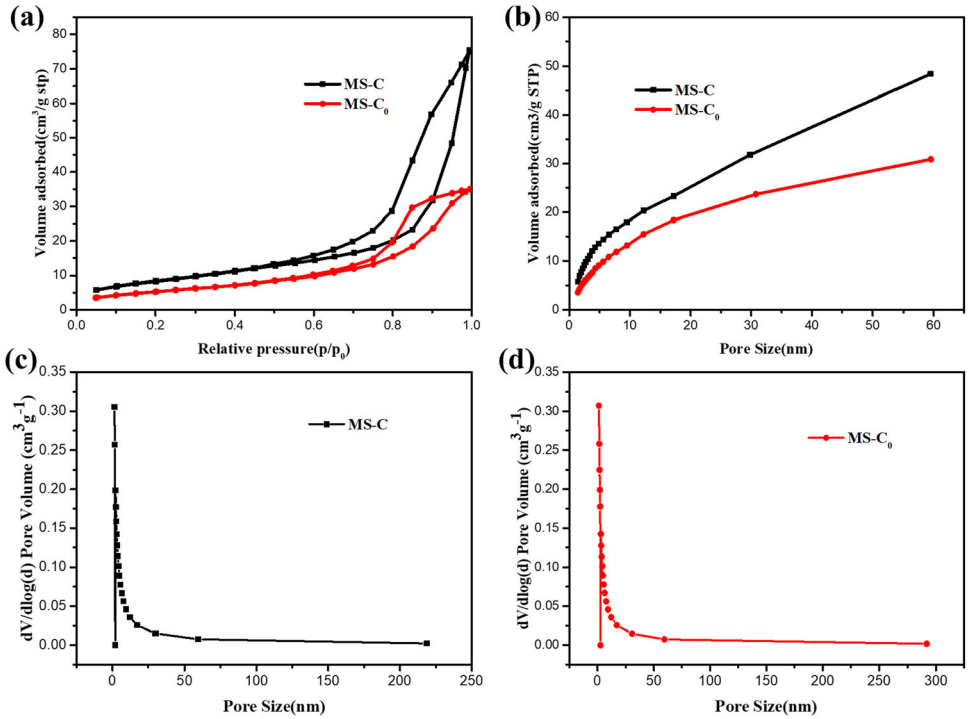

Fig. 13 (**a**) nitrogen adsorption isotherm of different samples, (**b**) cumulative pore volume, (**c**) (**d**) pore size distribution measured by BJH method

C showed even shorter blood clotting time and less blood loss than that of pure MSP, besides the less residue and a cleaner wound surface. The effective combination of mesoporous silica and cotton, high-specific surface area and porous structure of MSP, the flexibility and adsorption of cotton, all together contributed to the final excellent hemostatic performance of MS-C, besides improving the residual problem of hemostatic powder. Comparing with conventional hemostatic materials, MS-C has advantages of excellent hemostatic performance, strong adsorption, flexible structure, good biological safety and low cost. It was probably that MS-C had great potential for emergency hemostasis applications in the future.

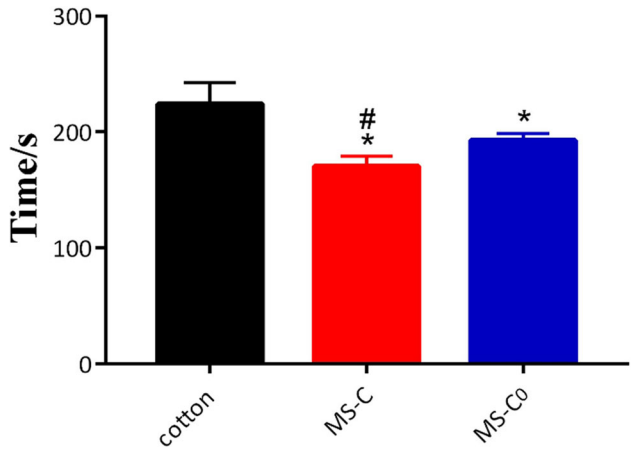

Fig. 14 In vitro clotting blood tests (CBT) of different samples, * indicates a significant difference from the blank control group, # indicates a significant difference between composite cotton and composite cotton-acetone (*P<0.05)

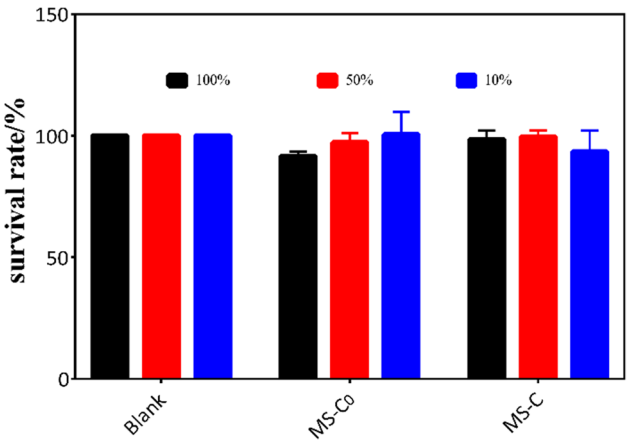

Fig. 15 Cell survival rate of different samples at leach liquor of 100%, 50% and 10%

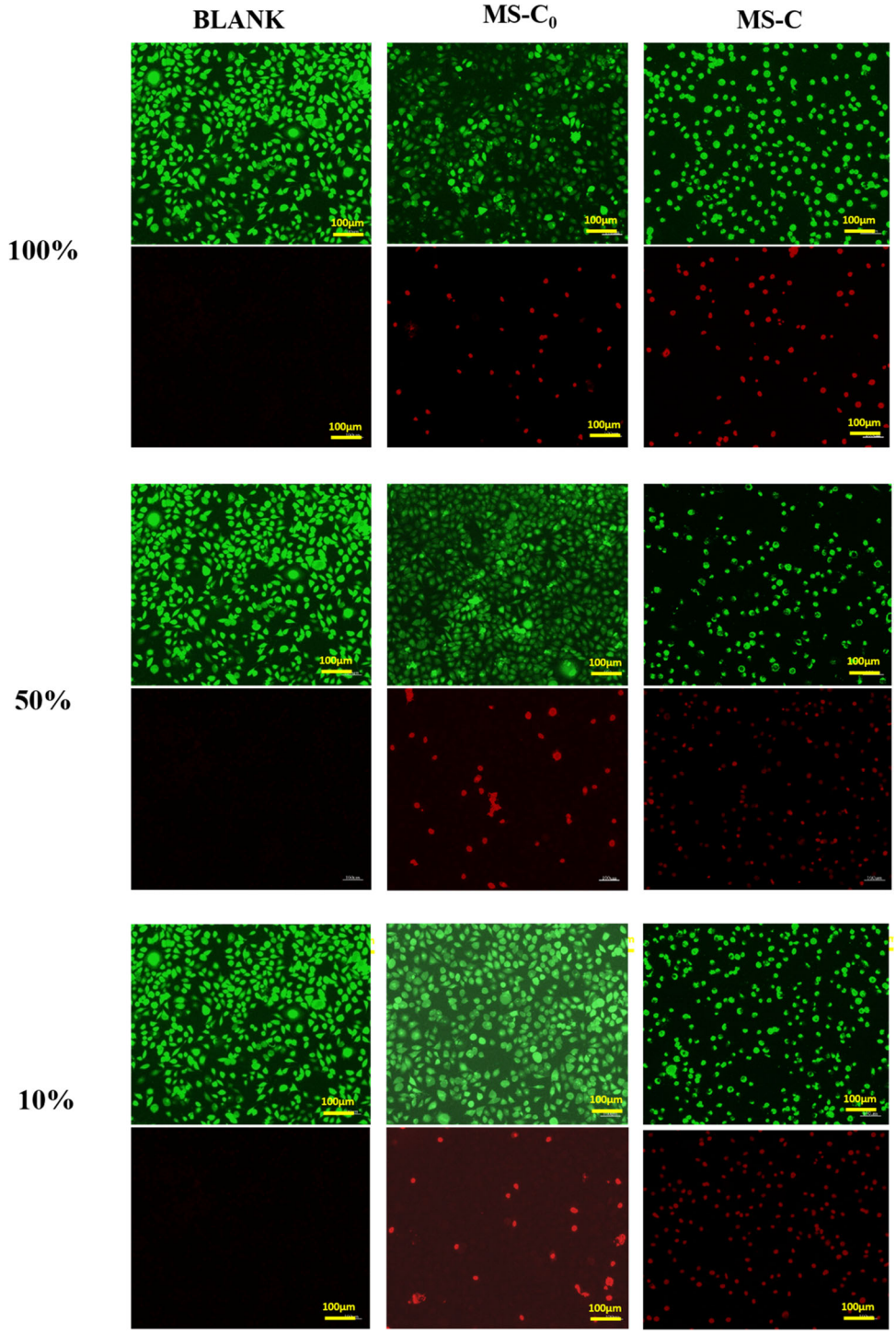

Fig. 16 Stained images of dead and living cells at leach liquor of 100%, 50% and 10%

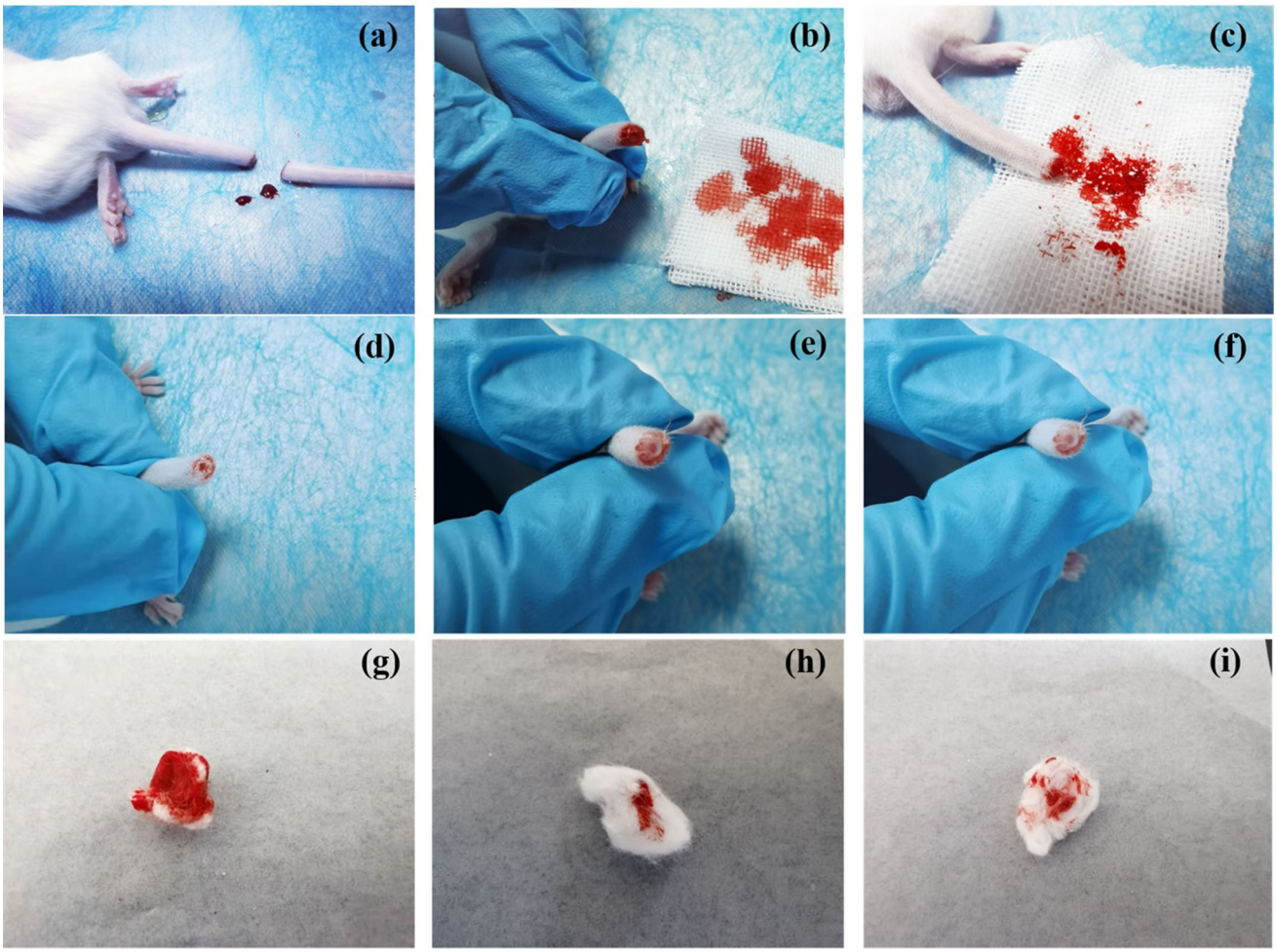

Fig. 17 Photos of various wounds and blood loss in a mouse tail truncation model: (**a**) Creation of the disturbance model of mouse, (**b**) Blank group after hemostasis, (**c**) Hard bleeding state after application of MSP, (**d**) Wound treated with MSP after hemostasis, (**e**) Wound treated with Cotton after hemostasis, (**f**) Wound treated with composite cotton after hemostasis, (**g**) Bleeding loss of wound treated with cotton, (**h**) Bleeding loss of wound treated with MS-C0, (**i**) Bleeding loss of wound treated with MS-C

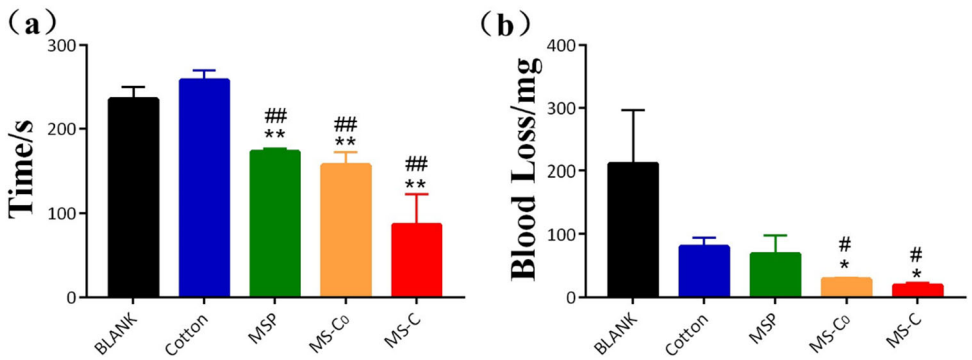

Fig. 18 The hemostatic time (**a**) and the blood loss (**b**) of different samples in the rat tail truncation model, * indicates a significant difference from the blank control group, # indicates a significant difference from the pure cotton group (*P<0.05,**P< 0.01)

Authors' contributions Zhuoran Zhang: Conceptualization, Methodology, Writing-Original Draft, Investigation and Resources.
Tao Liu: Investigation and Data Curation.
Zenghua Qi: Data Curation and Visualization.
Fan Li: Validation and Writing-Review&Editing.
Kun Yang, Sheng Ding, Song Lin, Feng Tian: Supervision.

Funding The authors gratefully acknowledge the support for this work from the Military Medical Innovation Project[20WQ045] and Technology Major Project Program[18ZXJMTG00070].

Data Availability All data generated or analysed during this study are included in this manuscript.

Declarations

Ethics Approval The animal experiment in this manuscript has passed ethical review, and the approval number is YSY-DWLL-2021018..

Consent to participate The authors have consented to participate in this study.

Consent for publication All authors have approved the future publication of this manuscript.

Conflict of interest The authors declare that they have no conflict of interest.

Disclosure of potential conflicts of interest Not applicable.

Research Involving Human Participants And/or Animals The animal experiment in this manuscript has passed ethical review, and the approval number is YSY-DWLL-2021018.

Authors' Information Not applicable.

Informed consent Not applicable.

References

1. Chen ZH, Han L, Liu CJ et al (2018) A rapid hemostatic sponge based on large, mesoporous silica nanoparticles and N-alkylated chitosan. Nanoscale 10:20234–20245
2. Stephanie A. Smith DVM, MS DACVIM((2009) The cell-based model of coagulation. Journal of Veterinary Emergency Critical Care 19(1):3–10
3. Pusateri AE, Holcomb JB, Kheirabadi BS et al (2006) Making sense of the preclinical literature on advanced hemostatic products. J Trauma 60(3):674–682
4. Yan TS, Cheng F, Wei XJ, Huang YD, He JM (2017) Biodegradable collagen sponge reinforced with chitosan/calcium pyrophosphate nanoflowers for rapid hemostasis. Carbohydrate Polymer 170:271–280
5. Zhang S, Xu QH, Tong L, Cao C, Ye H (2021) Current status and application of absorbable hemostatic materials. Chinese Journal of Tissue Engineering Research 25(10):1628–1634
6. Zhang H, Zhang DY, Lu ST, Li PW, Li SD (2018) Chitosan-Based Composite Materials for Prospective Hemostatic Applications. Mar Drugs 16(8):273–297
7. Lívia PS, Marília GDO, Antônio Luiz BP, Bruna RF, Marconi Eduardo SM (2008) Effects of laser therapy on experimental wound healing using oxidized regenerated cellulose hemostat. Photomed Laser Surg 26(1):10–13
8. Jerrold HL, Fania S, Kenichi AT, Roman MS (2012) Fibrinogen and hemostasis: a primary hemostatic target for the management of acquired bleeding. Anesthesia analgesia 114:261–273
9. Rorbert LW(1996)Tissue adhesive for battle field hemorrhage control[P]. ADB209674
10. Allison HA((2019) Hemorrhage Control: Lessons Learned From the Battlefield Use of Hemostatic Agents That Can Be Applied in a Hospital Setting. Critical Care Nursing Quarterly 42:165–172
11. Johnson D, Bates S, Nukalo S et al (2014) The effects of QuikClot Combat Gauze on hemorrhage control in the presence of hemodilution and hypothermia. Annals of Medicine Surgery 3:21–25
12. Rall JM, Cox JM, Songer AG, Cestero RF, Ross JD (2013) Comparison of novel hemostatic dressings with QuikClot combat gauze in a standardized swine model of uncontrolled hemorrhage. Trauma Acute Care Surg 75:S150–S156
13. Pourshahrestani S, Kadri NA, Zeimaran E, Towler MR (2019) Well-ordered mesoporous silica and bioactive glasses: promise for improved hemostasis. Biomaterials Science 7:31–50
14. Zheng CY, Zeng QY, Pimpi SaHu, Wu WD, Han k, Dong K, Lu TL (2020) Research status and development potential of composite hemostatic materials. J Mater Chem 8(25):5395–5410
15. Adam HS, Colville L, Keith P, Mark B (2013) Hemostatic dressings in prehospital care. Emerg Med J 30(10):784–789
16. Kheirabadi BS, Mace JE, Terrazas IB, Fedyk CG, Estep JS, Dubick MA, Blackbourne LH (2010) Safety evaluation of new hemostatic agents, Smectite granules, and kaolin-coated gauze in a vascular injury wound model in swine. Journal of Trauma-Injury Infection Critical Care 68(2):269–278
17. Alam HB, Uy GB, Miller D et al (2003) Comparative analysis of hemostatic agents in a sw ine model of lethal groin injury. Trauma 54(6):1077–1082
18. Pusateri AE, Delgado AV, Dick EJ, Martinez RS, Holcomb JB, Ryan KL (2004) Application of agranular mineral-based hemostatic agent (QuikClot) to reduce blood loss after grade V liver injury in swine. Trauma 57(3):555–562
19. Fathi P, Sikoraki M, Christodoulides K et al (2018) Zeolite-loaded alginate-chitosan hydrogel beads as a topical hemostat. Journal of Biomedical Materials Research Part B:Applied Biomaterials 106(5):1662–1671
20. Rahmat N, Abdullah AZ, Mohamed A (2010) A review: mesoporous Santa Barbara amorphous-15, types, synthesis and its applications towards biorefinery production[J]. American Journal of Applied Sciences 7(12):1579–1586
21. Manzano M, Vallet-Regí M (2010) New developments in ordered mesoporous materials for drug delivery. J Mater Chem 20:5593–5604
22. María VR, Luisa Ruiz GB, Isabel IB, José M. González C(2006) Revisiting silica based ordered mesoporous materials: medical applications. Journal of Materials Chemistry 16: 26–31
23. Liao S, He X (2015) Aplication of mesoporous materials on hemostasis. World Journal of Complex Medicine 1(4):347–349
24. Malmberg P, Nygren H (2002) A method for evaluating the influence of porosity on the early reactions of blood with materials. Biomaterials 23(1):247–253
25. Xv DY, Bi HD, Cai GJ, Xing X (2014) Hemostatic efficacies of mesoporous materials HW and ZSM-5: a comparative study. Academic Journal of Second Military
26. Sarah E, Baker AMS, Fan J, Shi QH, Nicholas S, Galen DS (2008) Blood Clot Initiation by Mesocellular Foams: Dependence on Nanopore Size and Enzyme. Immobilization Langmuir 24:4254–14260
27. Chen ZH, Li F, Liu CJ, Guan J, Hu X, Du G, Yao XP, Wu JM, Tian F (2016) Blood clot initiation by mesoporous silica nanoparticles:

dependence on pore size or particle size. Journal of Materials Chemistry B 4(44):7146–7154
28. Andreia F, Sandra G, Manuela RC et al(2021) Mesoporous silica nanoparticles with manganese and lanthanide salts: synthesis, characterization and cytotoxicity studies
29. Mayura L, Manohar C, Anirban G(2021) Synthesis, characterization and application development of ordered mesoporous silica in wastewater remediation. Journal of Porous Materials 1–13
30. Rozbeh R, Seyed Karim HD, Seyedeh MP (2021) Synthesis of MCM-41 mesoporous silica nanoparticles supported titanium dioxide-silver nanocomposite with excellent methanol electrooxidation performance. Fuel Cells 21(3):301–316
31. Wang J, Zhang CL, Bai YR, Li Q, Yang XZ (2021) Synthesis of mesoporous silica with ionic liquid surfactant as template. Mater Lett. doi:https://doi.org/10.1016/j.matlet.2021.129556
32. Svetlana M, Valentin V (1996) Deposition of zeolite A on vegetal fibers. Zeolites 16:31
33. Han KK, Ma L, Zhao HM, Li X, Chun Y, Zhu JH (2012) In situ synthesis of SBA-3/cotton fiber composite materials: A hybrid device for CO2 capture. Microporous Mesoporous Mater 151:157–162
34. Dekina SS, Romanovska II, Leonenko II, Yegorova AV (2015) Mucoadhesive Gel with Immobilized Lysozyme: Preparation and Properties. Biotechnologia Acta 8(1):109–109
35. Valtchev V, Mintova S, Vulchev I, Lazarova V1994). Influence of reactive radicals in cellulose fibres on the formation of zeolite coatings. Journal of the Chemical Society, Chemical Communications: 2087–2088. doi: https://doi.org/10.1039/C39940002087
36. Wan Y, Zhao DY (2007) On the Controllable Soft-Templating Approach to Mesoporous Silicates. Chem Rev 107(7):2821–2860
37. He Q, Zhang J, Shi J et al (2010) The effect of PEGylation of mesoporous silica nanoparticles on nonspecific binding of serum proteins and cellular responses. Biomaterials 31(6):1085–1092
38. Liu J, Yang QH, Zhao XS, Zhang L (2007) Pore size control of mesoporous silicas from mixtures of sodium silicate and TEOS. Microporous Mesoporous Mater 106:62–67
39. Simone GA, Silva LCC, Matosa JR (2016) Optimisation of SBA-15 properties using Soxhlet solvent extraction for template removal. Microporous Mesoporous Mater 234:277–286
40. Yu LS, Shang XQ, Chen H, Xiao LP, Zhu YH, Fan J(2019) A tightly-bonded and flexible mesoporous zeolite-cotton hybrid hemostat. Nature Communications 10: 1932
41. Wu S, Huang ZY, Yue JH et al (2015) The efficient hemostatic effect of Antarctic krill chitosan is related to its hydration property. Carbohydrate polymers 132:295–303
42. Kudela D, Smith SA, May-Masnou A et al (2015) Clotting activity of polyphosphate-functionalized silica nanoparticles[J]. Angewandte Chemie-International Edition 54(13):4018–4022
43. Zhao X, Guo BL, Wu H, Liang YP, Peter XM (2018) Injectable antibacterial conductive nanocomposite cryogels with rapid shape recovery for noncompressible hemorrhage and wound healing. Nature communications 9(1):2784. doi:https://doi.org/10.1038/s41467-018-04998-9
44. Zhao D, Feng J, Huo Q, Melosh N, Fredrickson GH, Chmelka BF, Stucky GD(1998)T riblock copolymer syntheses of mesoporous silica with periodic 50 to 300 angstrom pores. Science 279: 548–552
45. Tu J, Wang TX, Shi W et al (2012) Multifunctional ZnPc-loaded mesoporous silica nanoparticles for enhancement of photodynamic therapy efficacy by endolysosomal escape. Biomaterials 33(31): 7903–7914
46. Saulius B2012). Tissue factor structure and function. Scientifia (Cairo):964862
47. Hu HJ, Duan JC (2016) Influence of Nano-Silica on Blood Coagulation System and Research Progress. J Toxicol 30(5):395–389
48. Liao KH, Lin YS, Christopher WM, Christy LH (2011) Cytotoxicity of graphene oxide and graphene in human erythrocytes and skin fibroblasts. ACS Appl Mater Interfaces 3(7):2607–2615

Affiliations

Zhuoran Zhang [1] · Tao Liu [1,2] · Zenghua Qi [1] · Fan Li [1] · Kun Yang [1] · Sheng Ding [1] · Song Lin [1] · Feng Tian [1]

✉ Fan Li
vanadium_1981@163.com

[1] Institute of Medical Support Technology, Academy of Military Science, 300161 Tianjin, China

[2] Key Laboratory of Industrial Microbiology, Ministry of Education, College of Biotechnology, Tianjin University of Science and Technology, China International Science and Technology Cooperation Base of Food Nutrition/Safety and Medicinal Chemistry, 300457 Tianjin, China